IEEE Photonics Journal
An IEEE Photonics Society Publication

Open Access

LDPC-Coded Generalized Frequency Division Multiplexing for Intensity-Modulated Direct-Detection Optical Systems

Volume 11, Number 2, April 2019

Dong Guo
Wei Zhang
Feng Tian
Jianyang Shi
Kaihui Wang
Miao Kong
Junwen Zhang
Kai Lv
Deng'ao Li
Xiaolong Pan
Xiangjun Xin

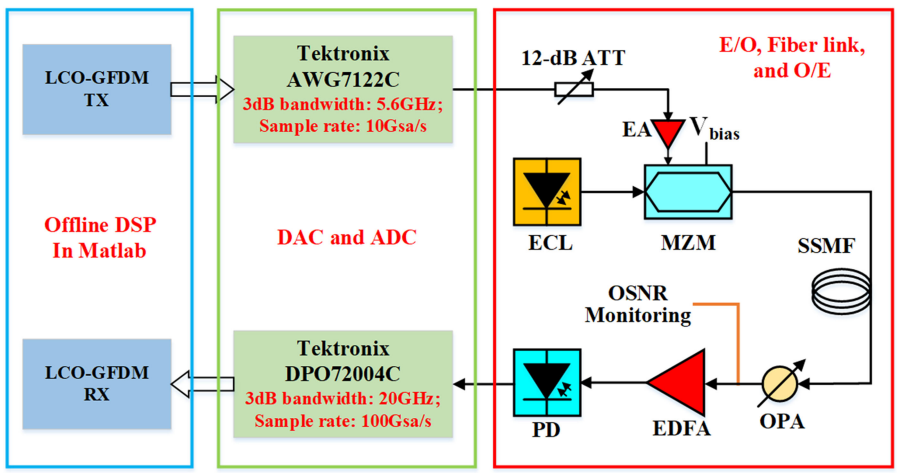

DOI: 10.1109/JPHOT.2019.2902607
1943-0655 © 2019 IEEE

LDPC-Coded Generalized Frequency Division Multiplexing for Intensity-Modulated Direct-Detection Optical Systems

Dong Guo [1,2] Wei Zhang,[3] Feng Tian [1,2] Jianyang Shi [4] Kaihui Wang [4] Miao Kong [4] Junwen Zhang [5] Kai Lv [1,2] Deng'ao Li,[6] Xiaolong Pan [1,2] and Xiangjun Xin[1,2]

[1]School of Electronic Engineering, Beijing University of Posts and Telecommunications, Beijing 100876, China
[2]Key Laboratory of Space-ground Interconnection and Convergence, Beijing University of Posts and Telecommunications, Beijing 100876, China
[3]China Academy of Space Technology, Beijing 100094, China
[4]Key Laboratory for Information Science of Electromagnetic Waves (MoE), Department of Communication Science and Engineering, Fudan University, Shanghai 200433, China
[5]ZTE (TX), Inc., Morristown, NJ 07960 USA
[6]College of Information Engineering, Taiyuan University of Technology, Taiyuan 030024, China

DOI:10.1109/JPHOT.2019.2902607

Manuscript received January 17, 2019; revised February 18, 2019; accepted February 27, 2019. Date of publication March 4, 2019; date of current version March 12, 2019. This work was supported in part by the National Natural Science Foundation of China under Grants 61425022, 61727817, 61522501, 61475024, 61475094, and 61605013; in part by the Beijing Nova Program under Grant Z141101001814048; in part by the Fundamental Research Funds for the Central Universities under Grant 2014RC0203, and in part by the Fund of State Key Laboratory of IPOC (BUPT). Corresponding author: Xiaolong Pan (e-mail: panxiaolong2018@126.com).

Abstract: In this paper, a low-density parity check (LDPC) coded GFDM with high-level modulation scheme is proposed for more flexible and advanced multicarrier modulation in intensity-modulated/direct-detection (IM/DD) optical systems. Then, we experimentally demonstrate an LDPC-coded GFDM with 16-quadrature amplitude modulation (16QAM) system transmitted over 20-km standard single-mode fiber at different symbol rates to verify the applicability of the proposed scheme. Furthermore, the proposed scheme with trellis-coded 32-quadrature amplitude modulation (TC-32QAM) has also been investigated and compared with the bit error rate (BER) performance with 16QAM-modulated condition. The results indicate that TC-32QAM-modulated GFDM method has a better performance than the 16QAM-modulated case. But with LDPC coding module added, the performance of the proposed system with TC-32QAM gets worse than that with 16QAM modulation. We also experimentally compare the proposed LDPC-coded scheme and the Turbo-coded scheme in the QAM-modulated GFDM IM/DD optical system. The results show the LDPC-coded optical (LCO-) GFDM scheme has lower power penalties and better BER performance. Moreover, the proposed LCO-GFDM scheme is applied in multiband transmission by optical simulation software, and the results show that multiband LCO-GFDM scheme has a better performance than that of LCO-OFDM scheme.

Index Terms: Generalized frequency division multiplex, low-density parity-check code, quadrature amplitude modulation, intensity-modulated/direct-detection systems.

1. Introduction

Due to exponential increase in triple play services and high data rate demands by the end users, multi-carrier modulation scheme is a very popular technique for optical access network. Orthogonal frequency division multiplexing (OFDM) plays a constructive role in multicarrier transmission which has great resistance to inter-symbol interference (ISI), high spectral efficiency and one-tap equalization [1]–[6]. However, several drawbacks of OFDM hinder its further and extensive application [7]–[11]. In the OFDM system, subcarriers are shaped by rectangular pulse shaping filter in time domain where the side lobes of Sinc(f) in frequency domain decompose slowly. Thus OFDM modulation system has high spectrum leakage and is very sensitive to carrier frequency offset. OFDM also has high peak-to-average power ratio (PAPR) and the overhead brought by the necessary cyclic prefix (CP) degrade the spectrum efficiency to a certain degree.

Advanced multi-carrier modulation formats have been investigated for the future communication system, such as Filter Bank Multicarrier (FBMC) / Universal Filtered Multicarrier (UFMC) / Generalized Frequency Division Multiplex (GFDM). Generally speaking, the key differences between these waveforms and OFDM is that they utilize filtering techniques, at the subcarrier and/or resource block level, to modify the spectral properties of their signals, leading to lower out-of-band (OOB) emissions [12]. Among those technologies, GFDM which is brought up by the group of 5GNOW in German, has some advantages in improving the system performance compared with OFDM technique, such as its lower out-of-band radiation and higher robustness against sampling time offset [12], [13]. In GFDM-based system, adjustable pulse shaping filter is required which has lower OOB radiation to the individual subcarriers, such as raised cosine (RC) filter, root-raised cosine (RRC) filter, Dirichlet filter [14]–[17]. A two-dimensional data structure is introduced to group data symbols across several subcarriers and time slots to blocks. Then tail-biting technique which can preserve circular properties across time and frequency domain is required to process these blocks. It should be noted that, the size of these blocks is a variable parameter and permits to implement long filters or to reduce the total number of subcarriers [18], [19]. Meanwhile, the position of adding CP is used before each frame instead of each symbol as in OFDM, which can effectively enhance the spectrum efficiency. GFDM has been experimentally proved to be more suitable in the passive optical network and LTE cellular system [12], [20]. Reference [12] demonstrates a universally filtered OFDM (UF-OFDM) and GFDM system with 10Gb/s PAM-4 signal applied in a converged 5G PON system, and Reference [20] investigates the benefits of the GFDM-based system compared with OFDM in LTE cellular system.

It is well known that forward error correction (FEC) code is widely adopted to recover data which can effectively improve the BER performance. Especially, Low-Density Parity-Check (LDPC) codes have showed its strong ability against burst symbol errors for the past few years. As to be a linear block code in essence, LDPC codes maps the information sequences into specific sequences through a generating matrix G or a sparse parity check matrix H, with redundancy added. Iterative decoding algorithm based on Belief-propagation (BP) are most widely utilized in the receiver [21]. Because of the sparse parity matrix, the information bits far away from each other are checked uniformly in the long code, which makes the continuous burst errors have little impact on the decoding, and the coding itself has the characteristics of anti-burst errors. In the field of coding theory, LDPC is able to achieve large coding gain with low decoding complexity.

LDPC-coded OFDM is proved to be an efficient coded modulation technique in optical transmission and mobile communication which can increase the spectrum efficiency and enhance the resistance to inter-symbol interference (ISI) [22], [23]. Several novel modulation schemes based on N-dimensional signal constellation mapping in coherent optical OFDM system are proposed and applied for ultra-high-speed optical transmission, which has high spectral efficiency and strong resistance against the channel impairment [24], [25]. The intensity-modulation/direct-detection (IM/DD) system with simple transceivers and low cost are widely utilized in optical wireless system and fiber-optic communication. Some devices (e.g., lasers and modulators) with excellent performance have been developed and applied in advanced optical transport experiments [26]–[29]. Lots of research have been done about IM/DD system based on OFDM [6], [30], [31]. Advanced multicarrier

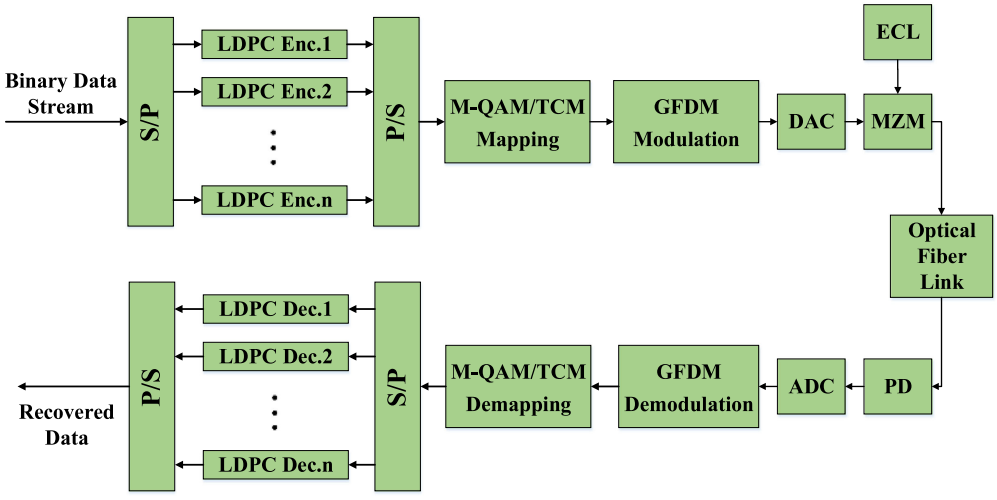

Fig. 1. The structure of LCO-GFDM system with M-QAM/TCM (Enc.: Encoder, Dec.: Decoder).

modulation like UFMC/FBMC also have been investigated with IM/DD transmission system in some radio-over-fiber (RoF) scenarios [32]–[34]. However, as far as we know, there are very few works that have studied the performance of the LDPC-coded GFDM for IM/DD optical systems. Considering that LDPC has strong ability for error correction with low decoding complexity in high noise environment and GFDM concentrated high-order modulation can provide high spectral efficiency, the research on combining these technologies is worth to be discovered. As to be an advanced multicarrier modulation technology, the proposed scheme will be applied for the large-capacity, high-speed and cost-effective communication, such as passive optical networks (PONs), Internet of things of 5G, and high-definition video dissemination.

In this paper, we propose a LDPC-coded optical GFDM (LCO-GFDM) IM/DD system with high-order modulation. The LCO-GFDM signal transmitted over 20-km standard single-mode fiber (SSMF) at 2.5-Gbaud and 5-Gbaud symbol rate is experimental demonstrated and analyzed. 16QAM and TC-32QAM formats are respectively investigated in our proposed system to achieve higher spectral efficiency. Furthermore, the performance improvement by using LDPC-coded GFDM and Turbo-coded GFDM in IM/DD optical system are compared under the same experimental setup. The results successfully demonstrated that the LCO-GFDM system with high-order modulation can achieve significant performance optimization and show its potential for the IM/DD optical systems. For further proving the advantages of our proposed LCO-GFDM modulation scheme, a multiband 16QAM-modulated LCO-GFDM IM/DD system is simulated. Results show that the system performance is mainly affected by fiber length, and the proposed LCO-GFDM scheme has better performance compared to the LCO-OFDM scheme in multi-band transmission.

2. Theoretical Investigation of the Proposed LCO-GFDM System

The block diagram of the proposed LCO-GFDM with high-level modulation scheme for IM/DD system is depicted in Fig. 1. The data sequences are transferred from serial to parallel (S/P) and encoded by multiple LDPC encoders. After parallel to serial (P/S) operation and M-QAM/TCM mapping, the modulated data are sent to the GFDM modulator and then upconverted to be a real-valued signal. A continuous wave (CW) output, from an external cavity laser (ECL), is modulated by a RF carrier, which carries the generated LDPC-coded GFDM signals and drives a Mach-Zehnder modulator. After transmitted across the optical fiber link, the LCO-GFDM signals are detected by a photo detector (PD) and captured by an oscilloscope. Data get recovered by the offline DSP, which mainly includes the GFDM demodulation module, M-QAM/TCM demappers and LDPC decoders.

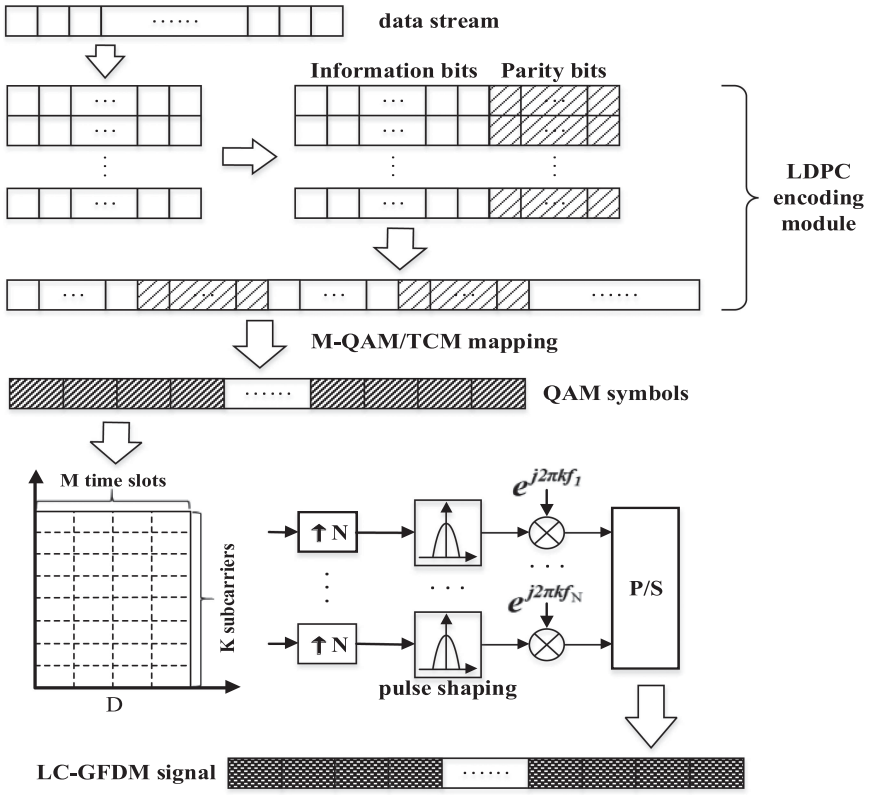

Fig. 2. Generation of LDPC-coded GFDM signal with M-QAM/TCM.

2.1 Transmitter of the LCO-GFDM System

Fig. 2 depicts the generation process of the LDPC-coded GFDM digital signal with high-level modulation.

2.1.1 LDPC-Coded 16QAM-Modulated GFDM System: As Fig. 2 shows, the random data are concurrently processed by multiple LDPC encoders with the aid of serial-to-parallel and parallel-to-serial transformation. The essential part of LDPC encoders, generating matrix G can be obtained by row and column transformation of parity-check matrix H achieved from IEEE 802.16e standard, where G is a $k \times n$ matrix and the code rate is k/n. Instead of encoding the binary data by H in general, such as lower upper (LU) decomposition coding and partially iterative coding algorithm, data directly multiply with matrix G which can reduce the pretreatment complexity of coding. The data sequences are encoded by the equation (1) as follows,

$$y_{l\times n} = mod\left(\left(\begin{pmatrix} x_{11} & \cdots & x_{1k} \\ \vdots & \ddots & \vdots \\ x_{l1} & \cdots & x_{lk} \end{pmatrix} \cdot G_{k\times n}, 2\right) \cdot l = \left\lceil \frac{length(data)}{k} \right\rceil \right. \tag{1}$$

where *mod* represents the modulo operation and the information bits are reshaped to the matrix $[x_{ij}]_{l\times k}$ by line. Afterwards, parity codes are added and interweaved with information bits by row. 16QAM with Gray mapping are then employed to transfer bits into symbols.

The linear symbol stream after high-level modulation is mapped to a data matrix $D = \{d_k(m)\}_{K\times M}$, where K and M represents the number of subcarriers and time-slots, and $d_k(m)$ represents the complex valued data symbols transmitted on the k_{th} subcarrier and the m_{th} time-slot, k = 0, . . . ,K − 1, m = 0, . . . ,M − 1 are given. After up-sampled by N and digital pulse shaping, the transmitted

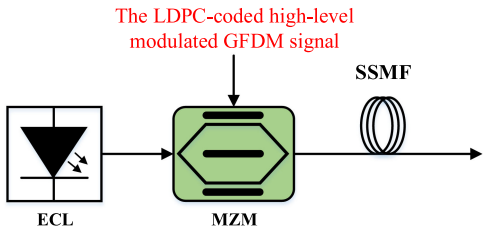

Fig. 3. Principle of the LDPC-coded high-level modulated GFDM signal generation.

LDPC-coded high-level modulated GFDM signal is generated and can be expressed as,

$$x[n] = \sum_{m=0}^{M-1} \sum_{k=0}^{K-1} [d_k[m]\delta[n - mN] \cdot \tilde{g}_{Tx}[n]] e^{j2\pi \frac{kn}{N}} \tag{2}$$

The subcarrier filter $\tilde{g}_{Tx}(n)$ can be achieved by circular shifting of $g_{Tx}(n)$ with a period of (n *mod* MN) which is used to facilitate tail biting at the transmitter. The Dirac function $\delta(n - mN)$ act as a time delay, and $e^{j2\pi \frac{kn}{N}}$ make the signal shifted by k/N in frequency domain. Dirichlet pulse shaping filter is utilized as the subcarrier filter, where a perfect rectangle function is applied in the frequency domain and its passband is centered at the DC bin. Dirichlet pulse shaping can not only get the same BER performance as OFDM system, but also can effectively suppress the OOB radiation. Compared with RC and RRC filter, Dirichlet pulse creates no self-interference. The phase-shifted characteristic matrix G is explained in the Reference [17], then we can get $g_{Tx}(n)$ by IFFT transformation for G.

$$[\bar{G}]_{k,l} = \begin{cases} 1, & 1 \le l < \lceil M/2 \rceil \\ e^{-j2\pi k/K}, & \lceil M/2 \rceil \le l < M \end{cases}, \qquad \forall 0 \le k < K \tag{3}$$

The GFDM transmitter include the frequency-domain implementation, frequency-domain convolution in time domain as element-wise vector multiplication, and the block circularity of matrices involved in modulation, which involves four steps: M sets of K-point inverse-DFTs (IDFTs), K sets of M-point DFTs, element-wise multiplication with a K $\times$ M matrix, and K sets of M-point IDFTs. The number of complex multiplications (CMs) can be calculated by the formula (4)

$$C_{GFDM} = M\frac{K}{2}\log_2 K + K\frac{M}{2}\log_2 M + KM + K\frac{M}{2}\log_2 M = KM\left(\frac{1}{2}\log_2 KM^2 + 1\right) \tag{4}$$

Supposing the GFDM and conventional OFDM transmitters use the same block size KM, the computational complexity of the conventional OFDM will be $M\frac{K}{2}\log_2 K + K\frac{M}{2}\log_2 M = \frac{1}{2}KM\log_2 KM$.

In the system, the high-level modulated LDPC-coded GFDM signal is up-converted and uploaded into an arbitrary waveform generator (AWG) to drive a MZM and modulate the CW output. Then the LDPC-coded 16QAM-modulated optical GFDM signal is generated, as shown in Fig. 3.

The proposed LCO-GFDM scheme is compared with the traditional OFDM technique and demonstrated in Table 1 with full details, where M represents the number of time-slots. It indicates that the LCO-GFDM scheme has shorter CP, higher spectrum efficiency and stronger ability to correct burst symbol errors.

2.1.2 LDPC-Coded TC-32QAM-Modulated GFDM System: It is common knowledge that trellis-coded modulation (TCM) technology combines modulation with coding and transmits information without bandwidth expansion, which can both have high efficiency, ability of correcting burst errors and is effectively applied in some special conditions, e.g., band-limited channels. So it is worth to be investigated with traditional high-level modulation formats applied in our proposed LCO-GFDM system. In TCM modulator, diversity mapping is a very important part that will not increase the transmission bandwidth and keep the Euclidean distance large enough to make the decision accuracy even if the redundancy is added. Taking the trellis-coded with 32-quadrature amplitude modulation (TC-32QAM) for example, the diversity mapping scheme of TC-32QAM is as Fig. 4

TABLE 1
System Properties

	traditional OFDM	LCO-GFDM
Subcarriers	Orthogonal	Non-orthogonal
Prototype filter	Rectangle	Dirichlet, RC, RRC
Convolution style	linear	circle
Cylic prefix	LCP	LCP/M
w or w/o FEC	w/o	w

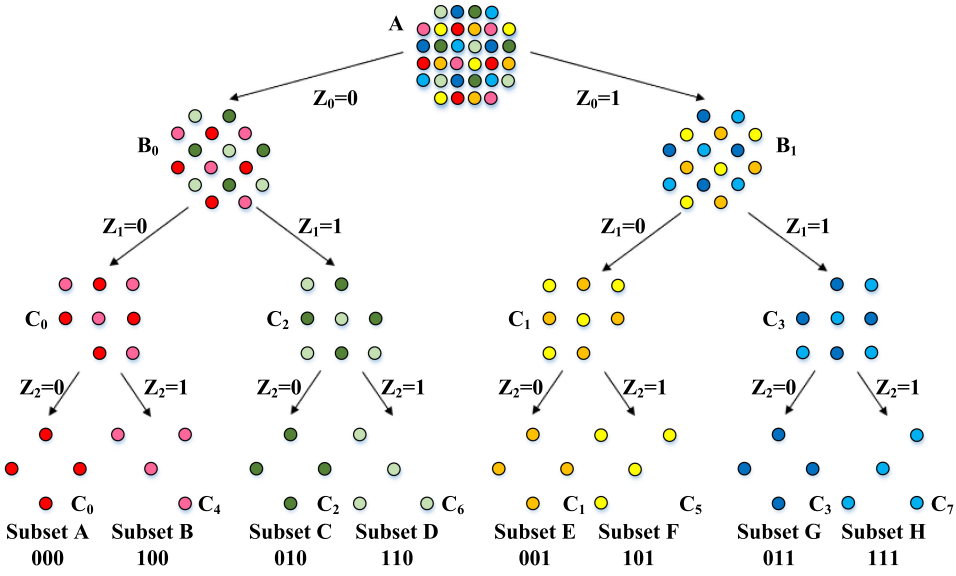

Fig. 4. Diversity mapping scheme of TC-32QAM.

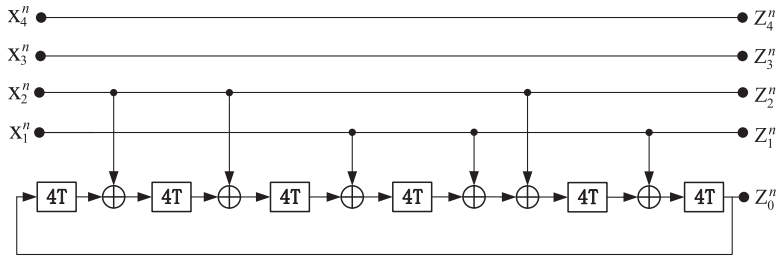

Fig. 5. The optimum structure of 64-state rate 4/5 convolutional encoder.

shows. Appropriate convolutional encoder should also be designed. Fig. 5 indicates the optimum structure of 64-state rate 4/5 convolutional encoder that is worth to be compared with traditional 16QAM formats. The system basically remains unchanged except that we use TC-32QAM modules instead of 16QAM blocks.

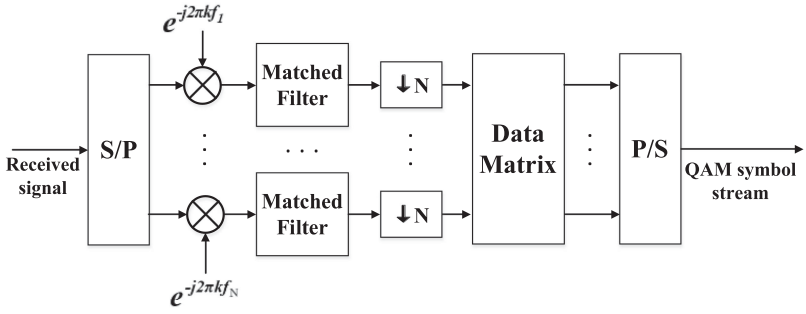

Fig. 6. Principle of GFDM demodulation system.

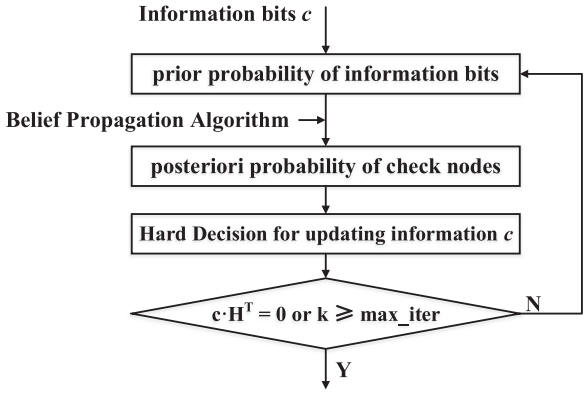

Fig. 7. Structure of LDPC decoder based on BP decoding algorithm.

2.2 Receiver of the LCO-GFDM System

After the fiber link and photodetector (PD) detection, the transmitted signal is firstly processed by GFDM demodulation module performed in frequency domain which is opposite to the modulation module, shown in Fig. 6. Suppose *y[n]* is the signal obtained at the receiver, then the resulting signal at $n = mN$ is given by the expression,

$$\tilde{d}_k[m] = \left(y[n]e^{-j2\pi\frac{kn}{N}}\right) \otimes g_{Rx}[n]|_{n=mN} \tag{5}$$

where $\otimes g_{Rx}[n]$ denotes circular convolution with matched filter (MF) relative to n which is essential for tail biting at the receiver. In frequency domain, the Equation (4) will be calculated by FFT and IFFT conversion flexibly. Except for the similar procedure at the transmitter, frequency-domain one-tap equalization which has $KM(\log_2 KM + 1)$ CMs is introduced at the receiver. So the total number of CMs at the GFDM receiver will be $KM(\frac{1}{2}\log_2 KM^2 + 1) + KM(\log_2 KM + 1)$. The conventional OFDM receiver implementation will take $\frac{1}{2}KM\log_2 KM + KM$ CMs.

After digital Rx-filtering, the signal is down-sampled turning sample index into QAM symbol index. The symbol index is then sent to the high-level modulation demappers. What needs to be illustrated is, in the TCM decoders, 'fast subset decoding' algorithm get the distance and distance index from the receiving point to the eight subsets firstly, which can reduce the complexity and storage space of subsequent Viterbi decoding algorithm. And then soft-decision Viterbi decoding module is employed by comparing the Euclidean distance with the receiving point and the various reference points. The closest point is identified and chosen.

The demapping outputs are fed to LDPC iterative decoders based on the belief propagation algorithm. The structure of iterative decoder is shown in Fig. 7, where the 'max_iter' represents the maximum number of iterations. Since the average of the random information is 0.5, different from

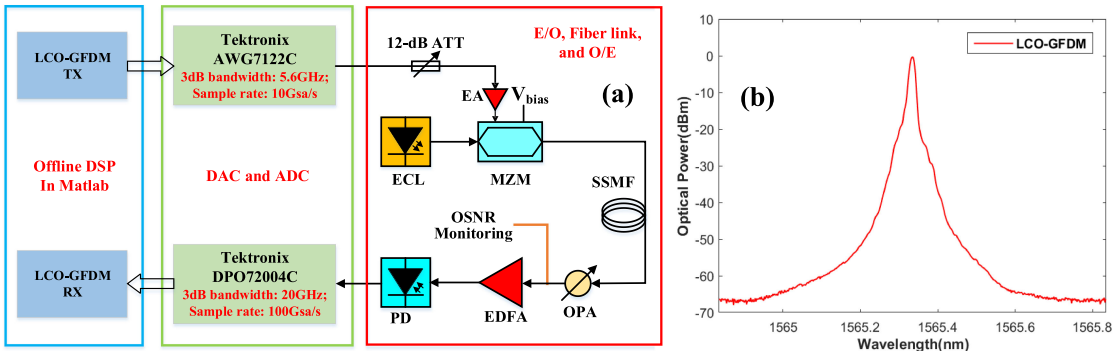

Fig. 8. (a) Experimental setup of the LCO-GFDM IM/DD system, (b) Optical spectrum of the LCO-GFDM signal. (EA: Electrical Amplifier, OPA: Optical power attenuator, EDFA: Erbium doped fiber amplifier).

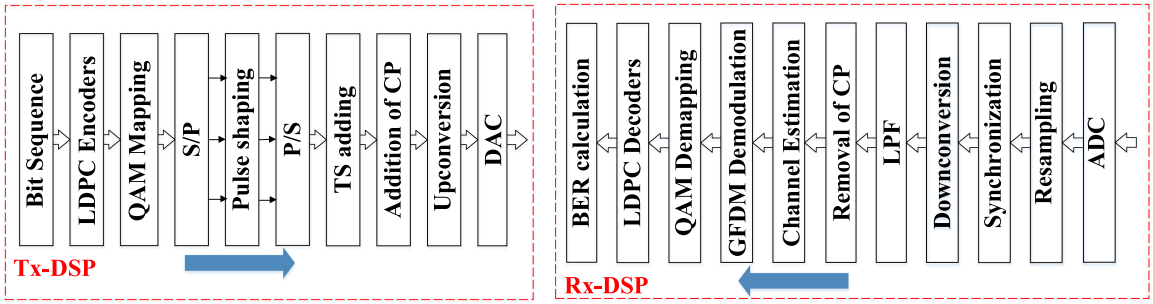

(a) (b)

Fig. 9. The Procedure of Offline DSP. (a) Transmitter (TX), (b) Receiver (RX).

the traditional BPSK signal, the prior probability of information bits should be modified as,

$$q_{ij}(1) = P_i = \mathrm{P}_r\left(x_i = 1|y\right) = \frac{1}{1 + e^{-2(y_i - 0.5)/\sigma^2}} \tag{6}$$

$$q_{ij}(0) = 1 - P_i = \mathrm{P}_r\left(x_i = 0|y\right) \tag{7}$$

where q_{ij}(b) indicates the probability that the i_{th} information node $c_i = b$ and other check nodes provide external information except the j_{th} check node. After calculating the posteriori probability of check nodes and information nodes successively, a hard decision is required to recover the sequence c of 0, 1. The iterative process of the BP algorithm is completely parallel. Moreover, the decoding process will directly break up if the condition is satisfied or the designed maximum number is reached.

3. Experimental Setup and Results

3.1 Experimental Setup

We experimentally demonstrated the proposed LCO-GFDM IM/DD systems with the setup shown in Fig. 8. The aforementioned LDPC-coded GFDM signal with high-order modulation is generated by Tx-DSP as Fig. 9(a) depicts. In detail, the random binary bits are coded by LDPC encoding module and then mapped to M-QAM/TCM symbols with Gray mapping. After serial-to-parallel (S/P) converting into a K $\times$ M data matrix (K $=$ 1024, M $=$ 20), a 1024-point IFFT is used to convert the signal from frequency domain to time domain, then digital pulse shaping is performed subcarrier-wise which is crucial to yield low out of band radiation. Simultaneously, the paralleled data are converted to serial stream. Afterwards, two training sequence (TS) symbols is added to the

data stream before symbol synchronization and zero-forcing equalization which can eliminate the impact of the channel. A single cyclic prefix (CP) for an entire GFDM block that contains multiple subsymbols is required. After 2-times up-sampling and up-conversion by a carrier frequency f_c, the data is uploaded into an arbitrary waveform generator (AWG) operating at 10 GSa/s to realize digital-to-analog conversion (DAC). An external cavity laser (ECL) is adopted to generate the optical carrier with a frequency of 191.52 THz. A Mach–Zehnder modulator (MZM) with a 3-dB bandwidth of 10 GHz which is biased at quadrature point and driven by electrical amplifier is used to modulate the optical carrier with the generated LCO-GFDM signal with high-order modulation. At the output of AWG, 12-dB electrical attenuator is required to limit the peak to peak voltage that can ensure the modulator working on its linear workspace after the signal amplified by EA. The net bit rate can be calculated by the equation (8),

$$\begin{aligned} Net\ bit\ rate &= 4\ bits/symbol \times 10\ GS/s(sampling\ rate) \times \frac{512(payload\ subcarriers)}{1024(total\ subcarriers)} \\ &\times \frac{1}{1+20\%(FEC overhead)} \times \frac{20(payloadsymbols)}{20(payloadsymbols)+2(trainingsymbols)+1(cyclic\ prefix)} \\ &\approx 14.49Gb/s \end{aligned} \tag{8}$$

After 20-km standard single mode fiber (SSMF) transmission, an optical power attenuator is adopted, which can act as a variable optical attenuator (VOA) monitoring the received of optical power (ROP). An Erbium doped fiber amplifier (EDFA), is used to amplify the generated LCO-GFDM signal and add amplified spontaneous emission (ASE) noise. Then, the received optical signal is converted into the electrical signal by a photodetector (PD) and captured by a real-time oscilloscope operating at 50 Gsa/s to realize analog-to-digital conversion (ADC). Following the ADC, the offline Rx-DSP are performed using MATLAB. The received data are down-sampled from 50 Gsa/s to 10 Gsa/s to match the ADC. Synchronization is employed using training sequence (TS) to align the up-converted data symbols. After being down-converted by f_c, the signal is filtered out with the high-frequency component following by the FIR low-pass filter (LPF). The second synchronization is required when the added CP is removed. After that, TS is used to do zero-forcing equalization for sake of channel estimation and phase recovery. After S/P converting and channel equalization, matched filter (MF) receiver is utilized to realize GFDM demodulation. Finally, data get recovered by M-QAM/TCM demappers and LDPC decoders.

3.2 Results and Discussion

The experimental results are measured from oscilloscope by varying the ROP with the help of optical power attenuator, and calculated by offline DSP algorithm. Fig. 10 shows the BER performances versus the received optical power (ROP) for un-coded/coded GFDM IM/DD system with high-level modulation transmitted through 20-km SSMF at 2.5-Gbaud and 5-Gbaud symbol rate.

3.2.1 LDPC-Coded 16QAM-Modulated GFDM IM/DD System: As shown in Fig. 10, when the measured BER is fixed at 1×10^{-3}, the ROPs of the LDPC-coded 16QAM-modulated GFDM system and the uncoded 16QAM-modulated GFDM system at 2.5-Gbaud are respectively -31.6 dBm and -24.2 dBm, which shows LDPC-coded scheme can get 7.4 dB improvement in this experiment. As the symbol rate increases to 5-Gbaud, the ROP is measured to be about -29.8 dBm for LDPC-coded 16QAM-modulated GFDM IM/DD system, which shows the applicability of the proposed model. The constellation diagrams of received signal are shown in Fig. 10(a).

In our experiment, there exists phase difference caused by up-conversion operation which trigger the phase rotation. By using TS to do the zero-forcing equalization, phase rotation can be eliminated as is shown in Fig. 11. The system performance and the symbol rate are restricted due to bandwidth limitation. Bandwidth limitation of our experiment is mainly because the restriction of essential components, such as the intensity modulator, electrical amplifier (EA), PD, and is need to be improved by increasing the spectral efficiency.

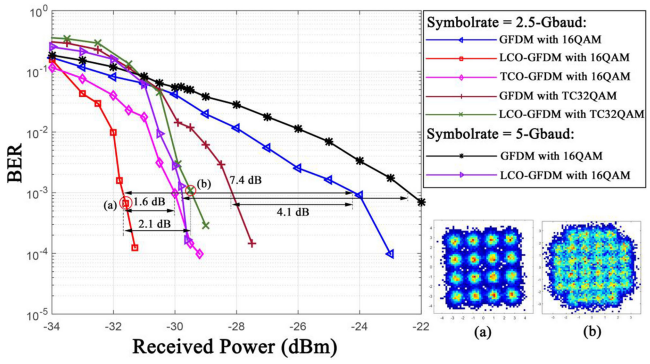

Fig. 10. The BER performance of GFDM IM/DD system with different modulation formats.

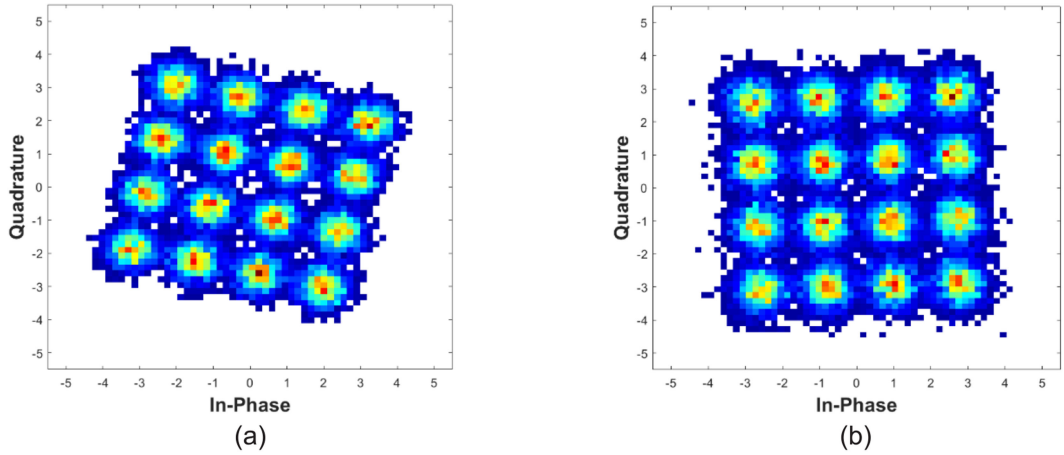

Fig. 11. Constellation after GFDM demodulation (a) before equalization. (b) after equalization.

3.2.2 LCO/TCO-GFDM IM/DD System With 16-QAM/TC-32QAM: When baud rate is fixed at 2.5-Gbaud and the experimental setup is all the same, the transmission performances of the optical GFDM IM/DD system after 20 km standard single mode fiber transmission are investigated in the following three cases:

1) As Fig. 10 shows, in our proposed GFDM IM/DD optical system without LDPC coding module, the ROPs are respectively -24.2 dBm and -28.3 dBm for 16QAM-modulated and TC-32QAM-modulated scheme at BER of 1×10^{-3}, which can prove the ability for correcting errors and 4.1 dB performance improvement of TC-32QAM technology. What needs to be illustrated is, TC-32QAM encoders with 64-state and the trellis code of rate 4/5 is adopted considering the coding gain, redundancy and time delay.
2) We also experimentally demonstrate the LDPC-coded TC-32QAM-modulated GFDM system with the same experimental setup. The constellation diagrams of received signal are shown in Fig. 10(b). From Fig. 10 we can get that the ROP of the TC-32QAM-modulated scheme is -29.5 dBm which shows worse receiver sensitivity by 2.1 dB than the LDPC-coded 16QAM-modulated GFDM system at BER of 1×10^{-3}. It's because the constellation in TC-32QAM formats are enlarged which increase the difficulty of the hard-decision part. BER performance get worse in lower OSNR condition and will cause interference in LDPC decoding. Take the high efficiency and considerable power penalty into account, TC-32QAM-modulated scheme can be applied in some band-limited channels.
3) By using Recursive system convolutional coder (RSC), random interleaver and soft output iterative decoding algorithm, Turbo coding module is realized and applied in our proposed

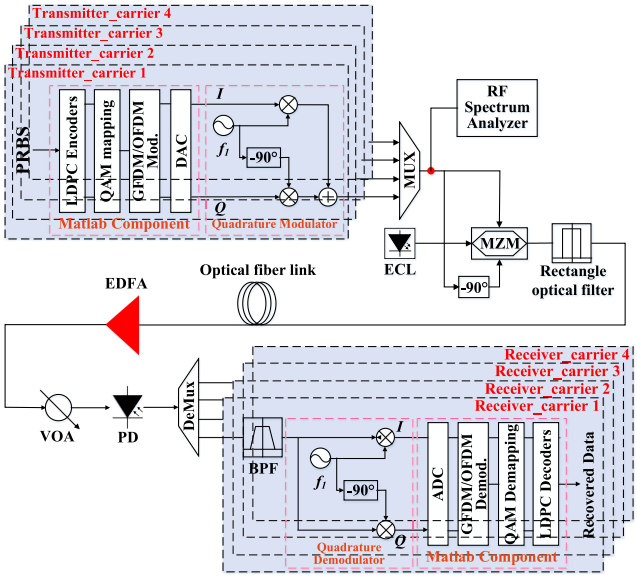

Fig. 12. Block diagram of multi-band 16QAM-modulated LCO-GFDM IM/DD system.

system as an extension study. Turbo codes is also widely used in coding fields because it is almost as close to the Shannon limit as that of LDPC codes. However, it is susceptible to be interfered by low code weight codes and convolvers, which increases the complexity and reduces the BER performance. Turbo-coded 16QAM-modulated GFDM for IM/DD optical system is successfully achieved. As shown in Fig. 10, the ROP at the BER of 1×10^{-3} was measured to be about -30.0 dBm. It shows that Turbo-coded scheme has about 1.6 dB power penalty compared to LDPC-coded scheme. Therefore, LDPC codes is more suitable in our proposed system.

4. Simulation of Multi-Band Transmission Based on the LCO-GFDM Scheme

GFDM systems have better bandwidth roll-off performance than OFDM, which can decrease the inter-carrier interference (ICI) and improve the performance in multiband transmission. For further proving the advantages of our proposed LCO-GFDM modulation scheme, a multiband 16QAM-modulated LCO-GFDM IM/DD system is demonstrated by an optical simulation software called optisystem. As shown in Fig. 12, four strings of data are represented by the 10Gb/s pseudorandom bit sequence generated from the PRBS. The electrical LDPC-coded 16QAM-GFDM/OFDM signal is generated by matlab component in the transmitter and is converted from baseband to RF band by a quadrature modulator. In this simulation, four quadrature modulators at different center frequency of 10/13/16/19 GHz are used to realize the multi-band transmission by a 4×1 multiplexer. The output electrical spectrum for the LDPC-coded GFDM signal is displayed by a RF spectrum analyzer, as shown in Fig. 13. Simulation results show that GFDM-based system has about 20dB OOB suppression compared to OFDM-based system. A LiNb MZM is used to modulate a CW laser with the generated LCO-GFDM signal. After an optical band pass filter (OBPF) filtering out the out-of-band noise and fiber transmission, the signal will be amplified and detected. And then, the signal is split into four parts and each part will pass a BPF with specified center frequency at f_1–f_4 respectively. Then the RF signal is down-converted to the baseband by a quadrature demodulator and data get recovered by matlab component including ADC, GFDM demodulation, 16QAM demapping and LDPC decoding.

In the simulation, the fiber parameters are set according to SSMF, the attenuation is 0.2 dB/km, the dispersion coefficient is 16 ps/nm/km. By sweeping the fiber length from 20 km to 50 km, the

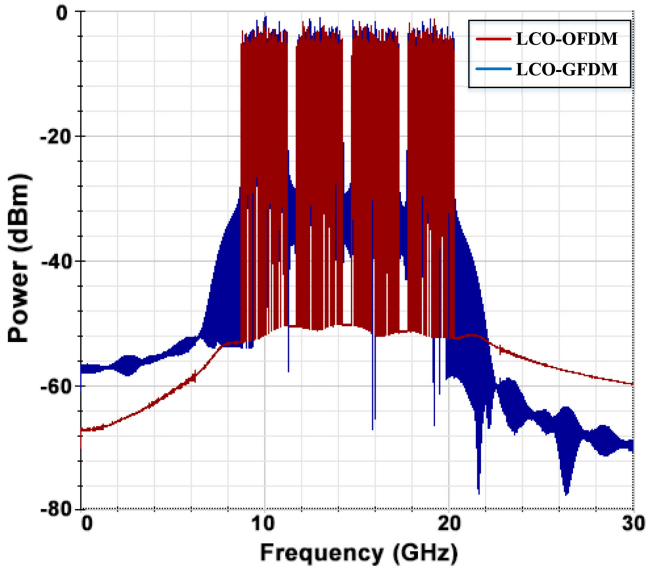

Fig. 13. Electrical spectrum for the multi-band 16QAM-modulated LCO-GFDM/OFDM signals.

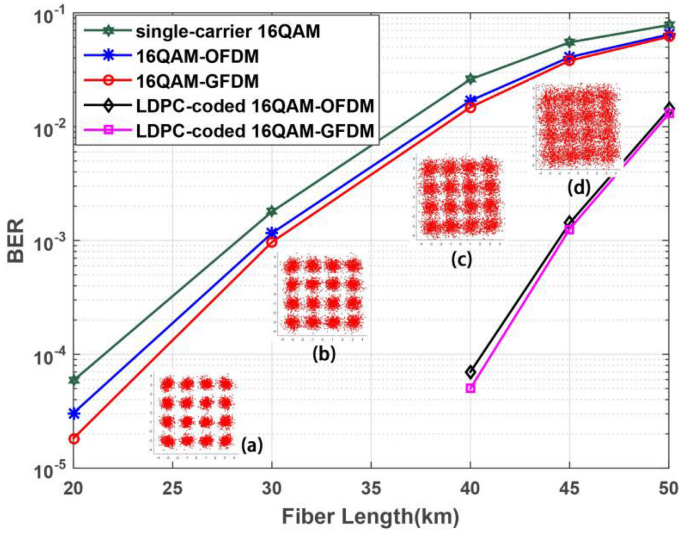

Fig. 14. BER performance versus fiber length at 2.5-Gbaud (for carrier2). (a) 20 km-,(b) 30 km-, (c) 40 km-, (d) 50 km-, constellations.

BER performance and constellations are calculated and illustrated in Fig. 14, and it shows that the multi-band 16QAM-modulated LCO-GFDM/OFDM IM/DD system was successfully realized at BER of 4.6×10^{-5} when the signal transmit over 40 km fiber. It can be observed that system performance gets worse with the fiber length increasing, which is mainly affected by the fiber dispersion. The performance of single-carrier 16QAM system is slightly worse than that of 16QAM-OFDM/GFDM system because it cannot effectively resist to the inter-symbol interference (ISI). Besides, multi-band transmission of the LCO-GFDM signal have lower BER than that of LCO-OFDM, which indicates the benefits of our proposed scheme.

To verify the relevance of the proposed scheme, longer SSMF distance is performed in the simulation as Fig. 15 shows. The new fiber link is composed of N spans of length $L = 36$ km, consisting of 30 km D_+ fibers followed by 6 km D_- fibers and EDFA. The fiber Parameters are listed in

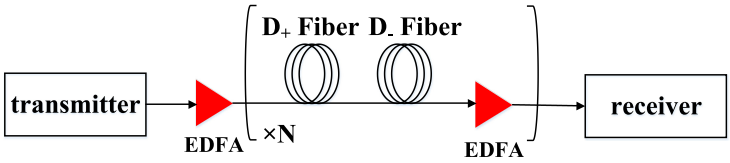

Fig. 15. System setup with N spans fiber link.

TABLE 2
Fiber Parameters

	D_+ Fiber	D- Fiber
Fiber length	30	6
Dispersion [ps/(nm·km)]	16	-80
Dispersion slope [ps/(nm2·km)]	0.075	0.075
Effective cross-sectional area [μm2]	80	80
Nonlinear refractive index [m2/W]	2.6×10-20	2.6×10-20
Attenuation coefficient [dB/km]	0.2	0.2

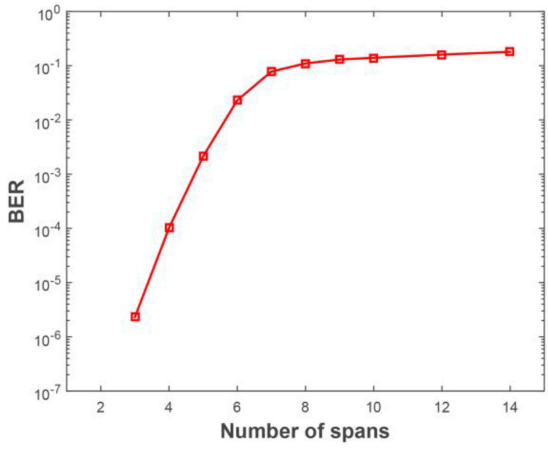

Fig. 16. BER curve versus number of spans for LCO-GFDM optical IM/DD system.

Table 2. The length of D+ fibers is five times of D- fibers so that the effect of chromatic dispersion can be ignored without corresponding algorithm added in the receiver. In this case, channel distortion is mainly introduced by some nonlinear effect such as self-phase modulation (SPM) and cross-phase modulation (XPM). When the optical power into PD is fixed at 0-dBm, the BER curve versus number of spans for LCO-GFDM optical IM/DD system is shown in Fig. 16.

5. Conclusions

In this paper, we have proposed a LDPC-coded GFDM scheme with high-order modulation formats for intensity-modulated/direct-detection optical systems, and experimentally demonstrated its feasibility and performance. The experimental results show that the received optical power of LDPC-coded 16QAM-modulated GFDM system after 20 km SSMF transmission at 2.5-Gbaud and 5-Gbaud are respectively -31.6 dBm, and -29.8 dBm at the BER of 1×10^{-3}. When the baud rate is fixed at 2.5-Gbaud, LDPC-coded scheme can provide 7.4 dB coding gain than the uncoded scheme for 16QAM-modulated GFDM IM/DD optical system. And the TC-32QAM-modulated GFDM

system has 4.1 dB performance improvement than the 16QAM-modulated condition, while the performance of LDPC-coded TC-32QAM-modulated GFDM system gets worse by 2.1 dB than that of LDPC-coded 16QAM GFDM system. Besides, Turbo-coded 16QAM-modulated GFDM system is investigated to be compared with our proposed LDPC-coded GFDM system, and shows to have 1.6 dB power penalty. The results indicate that our proposed LCO-GFDM with high-level modulation scheme for IM/DD system can achieve considerable performance such as high spectral efficiency and significant coding gain, and show the potential for future IM/DD optical systems. The simulation about the multi-band LCO-GFDM transmission is successfully realized at BER of 4.6×10^{-5} when the signal transmit over 40 km fiber. The results show that fiber dispersion will significantly affect system performance and the proposed LCO-GFDM scheme have lower BER than LCO-OFDM in multi-band transmission.

References

[1] N. Cvijetic, "OFDM for next-generation optical access networks," *J. Lightw. Technol.*, vol. 30, no. 4, pp. 384–398, Feb. 2012, doi: 10.1109/ JLT.2011.2166375.

[2] J. Zhou *et al.*, "Interleaved single-carrier frequency-division multiplexing for optical interconnects," *Opt. Exp.*, vol. 25, no. 9, pp. 10586–10596, May 2017, doi: 10.1364/OE.25.010586.

[3] F. Li, X. Li, J. Zhang, and J. Yu, "Transmission of 100-Gbps VSB DFT-spread DMT signal in short-reach optical communication systems," *IEEE Photon. J.*, vol. 7, no. 5, Oct. 2015, Art. no. 7904307.

[4] F. Li, J. Zhang, J. Yu, and X. Li, "Transmission and reception of PDM dual-subcarrier coherent 16QAM-OFDM signals," *Opt. Fiber Technol*, vol. 26, pp. 201–205, Dec. 2015, doi: 10.1016/j.yofte.2015.09.006.

[5] F. Li, X. Li, and J. Yu, "Performance comparison of DFT-spread and pre-equalization for 8 × 244.2-Gbps PDM-16QAM-OFDM," *J. Lightw. Technol.*, vol. 33, no. 1, pp. 227–233, Jan. 2015.

[6] J. Zhou and Y. Qiao, "Low-PAPR asymmetrically clipped optical OFDM for intensity-modulation direct-detection systems," *IEEE Photon. J.*, vol. 7, no. 3, Jun. 2015, Art. no. 7101608.

[7] J. Zhou *et al.*, "256-QAM interleaved single carrier FDM for short-reach optical interconnects," *IEEE Photon. Technol. Lett.*, vol. 29, no. 21, pp. 1796–1799, Nov. 2017, doi: 10.1109/LPT.2017.2752215.

[8] X. Li, J. Xiao, F. Li, Y. Xu, L. Chen, and J. Yu, "Large capacity optical wireless signal delivery At W-band: OFDM or single carrier?," in *Proc. Opt. Fiber Commun. Conf. Exhib.*, Anaheim, CA, USA, Mar. 2016, Paper TU2B.6.

[9] X. Li *et al.*, "Real-time demonstration of over 20Gbps V- and W-band wireless transmission capacity in one OFDM-RoF system," in *Proc. Opt. Fiber Commun. Conf. Exhib.*, Los Angeles, CA, USA, Mar. 2017, Paper M3E.3.

[10] J. Shi, Y. Zhou, Y. Xu, J. Zhang, J. Yu, and N. Chi, "200-Gbps DFT-S OFDM using DD-MZM-based twin-SSB with a MIMO-volterra equalizer," *IEEE Photon. Technol. Lett.*, vol. 29, no. 14, pp. 1183–1186, Jul. 2017.

[11] B. Liu, L. Zhang, X. Xin, and J. Yu, "Robust generalized filter bank multicarrier based optical access system with electrical polar coding," *IEEE Photon. J.*, vol. 8, no. 5, Oct. 2016, Art. no. 7906507.

[12] C. Browning *et al.*, "5G wireless and wired convergence in a passive optical network using UF-OFDM and GFDM," in *Proc. IEEE Int. Conf. Commun. Workshops*, Paris, France, May 2017, pp. 386–392.

[13] N. Michailow *et al.*, "Generalized frequency division multiplexing for 5th generation cellular networks," *IEEE Trans. Commun.*, vol. 62, no. 9, pp. 3045–3061, Sep. 2014.

[14] N. Michailow and G. Fettweis, "Low peak-to-average power ratio for next generation cellular systems with generalized frequency division multiplexing," in *Proc. Int. Symp. Intell. Signal Process. Commun. Syst.*, Naha, Japan, Nov. 2013, pp. 651–655.

[15] N. Michailow, S. Krone, Mi. Lentmaier, and G. Fettweis, "Bit error rate performance of generalized frequency division multiplexing," in *Proc. Veh. Technol. Conf.*, vol. 48, no. 2, pp. 1–5, Sep. 2012.

[16] P. C. Chen, B. Su, and Y. Huang, "Matrix characterization for GFDM: Low complexity MMSE receivers and optimal filters," *IEEE Trans. Signal Process.*, vol. 65, no. 18, pp. 4940–4955, Sep. 2017.

[17] M. Matthé, N. Michailow, I. Gaspar, and G. Fettweis, "Influence of pulse shaping on bit error rate performance and out of band radiation of generalized frequency division multiplexing," in *Proc. IEEE Int. Conf. Commun. Workshops*, Sydney, NSW, Australia, Jun. 2014, pp. 43–48.

[18] N. Michailow, I. Gaspar, S. Krone, M. Lentmaier, and G. Fettweis, "Generalized frequency division multiplexing analysis of an alternative multi-carrier technique for next generation cellular systems," in *Proc. Int. Symp. Wireless Commun. Syst.*, Paris, France, Aug. 2012, pp. 171–175.

[19] G. Fettweis, M. Krondorf, and S. Bittner, "GFDM-generalized frequency division multiplexing," in *Proc. IEEE 69th Veh. Technol. Conf.*, Barcelona, Spain, Apr. 2009.

[20] M. Danneberg, R. Datta, A. Festag, and G. Fettweis, "Experimental testbed for 5G cognitive radio access in 4G LTE cellular systems," in *Proc. IEEE 8th Sensor Array Multichannel Signal Process. Workshop*, A Coruna, Spain, Jun. 2014, pp. 321–324.

[21] J. Chen and MPC Fossorier, "Near optimum universal belief propagation based decoding of low-density parity check codes," *IEEE Trans. Commun.*, vol. 50, no. 3, pp. 406–414, Aug. 2002, doi: 10.1109/26.990903.

[22] I. B. Djordjevic and B. Vasic, "LDPC-coded OFDM in fiber-optics communication systems," *J. Opt. Netw.*, vol. 7, no. 3, pp. 217–226, Mar. 2008.

[23] I. B. Djordjevic and H. G. Batshon, "LDPC-coded OFDM for heterogeneous access optical networks," *IEEE Photon. J.*, vol. 2, no. 4, pp. 611–619, Aug. 2010.

[24] I. B. Djordjevic, M. Arabaci, L. Xu, and T. Wang, "Generalized OFDM (GOFDM) for ultra-high-speed optical transmission," *Opt. Exp.*, vol. 19, no. 7, pp. 6969–6979, 2011.
[25] I. B. Djordjevic, H. G. Batshon, L. Xu, and T. Wang, "Four-dimensional optical multiband-OFDM for beyond 1.4 Tb/s serial optical transmission," *Opt. Exp.*, vol. 19, no. 2, pp. 876–882, 2011.
[26] S. Chen *et al.*, "Electrically pumped continuous-wave iii–v quantum dot lasers on silicon," *Nature Photon.*, vol. 10, no. 5, pp. 307–322, 2016.
[27] K. Xu, "Monolithically integrated Si gate-controlled light-emitting device science and properties," *J. Optics*, vol. 20, no. 2, Jan. 2018, Art. no. 024014.
[28] K. Xu *et al.*, "Light emission from a poly-silicon device with carrier injection engineering," *Mater. Sci. Eng.: B*, vol. 231, pp. 28–31, May 2018.
[29] H. Elghazi, A. Jorio, and I. Zorkani, "Analysis of temperature and 1 mev proton irradiation effects on the light emission in bulk silicon (NPN) emitter-base bipolar junctions," *Opt. Commun.*, vol. 280, no. 2, pp. 278–284, 2007.
[30] L. Zhang, B. Liu, and X. Xin, "Secure optical generalized filter bank multi-carrier system based on cubic constellation masked method," *Opt. Lett.* vol. 40, no. 12, pp. 2711–2714, Jun. 2015.
[31] P. M. Anandarajah, R. Zhou, C. Browning, and L. P. Barry, "Performance investigation of IMDD compatible SSB-OFDM systems based on optical multicarrier sources," *IEEE Photon. J.*, vol. 6, no. 5, Oct. 2014, Art. no. 7903110.
[32] L. Zhang, S. Xiao, M. Bi, L. Liu, and X. Chen, "FFT-based universal filtered multicarrier technology for low overhead and agile datacenter interconnect." *Proc. Int. Conf. Transparent Opt. Netw.*, 2016, pp. 1–4.
[33] W. C. Yuan, C. Zhang, and K. Qiu. "Transmission performance of NOMA and FBMC-based IM/DD RoF-5G communications." *Proc. Int. Topical Meeting Microw. Photon.*, 2017, pp. 1–4.
[34] J. Wang *et al.*, "Delta-sigma modulation for digital mobile fronthaul enabling carrier aggregation of 32 4G-LTE / 30 5G-FBMC signals in a single-λ 10-Gb/s IM-DD Channel," in *Proc. Opt. Fiber Commun. Conf. Exhib.*, Anaheim, CA, USA, Mar. 2016, Paper W1H.2.